OPEN ACCESS
Haya: The Saudi Journal of Life Sciences
Abbreviated Key Title: Haya Saudi J Life Sci
ISSN 2415-623X (Print) |ISSN 2415-6221 (Online)
Scholars Middle East Publishers, Dubai, United Arab Emirates
Journal homepage: http://scholarsmepub.com/haya/

Original Research Article

Characterization of Syzygium Cumini Silver Nanoparticles (SCSNPS) and Analyzing Their Effect on Glucose Induced Cardiac Stress

Ajay Kumar Sahu[1], Dr. Rupali Sinha[2], Prangya Paramita Acharya[3], Deepthi Kiran k[1]
[1]Department of Microbiology, Bangalore University, Bangalore, Karnataka, India
[2]Department of Botany, Purvanchal University, Uttar Pradesh, India
[3]Department of Biotechnology, Sambalpur University, Odisha, India

***Corresponding author:** Ajay Kumar Sahu
| **Received:** 10.04.2019 | **Accepted:** 19.04.2019 | **Published:** 30.04.2019
DOI:10.21276/haya.2019.4.3.3

Abstract

Photosynthesis or green synthesis of silver nanoparticles has been shown an ecofriendly and cost effective approach with a great significance of biomedical Applications. Plant extracts may act both as reducing agents and stabilizing agents in the nanoparticles formation. We therefore synthesized silver nanoparticles using *Syzygium cumini* methanol seed extract which is found to be most enriched in Phytonutrients, and had strong anti-glycoxidative potential. In this chapter, the Characterization of silver nanoparticles of *S.cumini* (ScSNPs) methanol seed extract was performed and their role on glucose stressed cardiac cells was studied. Nanoparticles synthesis is based upon its size, shape, disparity and surface area. After mixing with silver nitrate solution the colour changes from yellow to dark Brown confirming the formations of nanoparticles. This colour change is due to the Excitation of surface plasmon vibrations. We have synthesized the silver nanoparticles after 48 h of incubation but sometimes it takes more/less time depends upon the rateof bio-reduction of silver ion due to the presence of reactivity of enzymes and components exist in plant extract. The silver ions bind to the secondary metabolites in*S. cumini* and getting reduced. This complex of silver ion and metabolite interacts with other complexes and contributes to the formation of silver nanoparticle, which is a critical phenomenon and affected by pH, temperature, concentration and electrochemical gradient of silver ion. The plasmon resonance is acombined resonance of the conducting electrons of silver nanoparticles and scatteroptical light elastically with significant efficiency our study reveals that the polyphones and amines in *S. cumini* contribute to the formation of synthesis of silver nanoparticles and might go through a two-step redox process.

AgI + R´-OH → Ag0 + R´= O (i)
AgNO3 + 3NR3 → Ag0 + 3NR3+ (ii)

Keywords: Green synthesis of silver nanoparticles, UV-Vis spectroscopy, SEM analysis, Zeta potential analysis, DLS analysis, XRD analysis, FTIR analysis, DPPH assay, ABTS assay, MTT assay, Morphological analysis, Nuclear morphological analysis.

INTRODUCTION

Nanotechnology is an emerging area of research due to its wide applications in pharmaceuticals and medicinal fields [1, 2]. The usage of plant products for the synthesis of nanoparticles includes a new aspect of therapeutics in the medicinal fields. The synthesis and characterization of nanoparticles is the most imperative and critical [2, 3].

Process as proper selection of size and shape of nanoparticles is significant to control over many of the physico-chemical properties [15, 16]. Nanoparticles treatment with the normal body weight, protein levels, and high-density lipoprotein were monitored in streptozotocin-induced diabetic rats, Silver nanoparticles (SNPs) have recently been studied for their antidiabetic potential where a significant reduction in blood glucose level was observed in diabetic rats and also found to be beneficial in delayed diabetic wound healing [3, 4].

Silver Nanoparticles have wide application in pharmaceutical industry and biomedical science [5, 7]. Among the noble metals, silver is beneficial because it is used as a health Additive in traditional medicine due to its exclusive properties such as catalytic Activity [12, 18], good conductivity, chemically stable, surface enhanced Raman scattering, Antimicrobial activity and increased oral bio-availability, recent studies Illustrated that the synthesis of silver nanoparticles using biological route or plant Extracts is beneficial against the pathological conditions [7, 8]. Illustrated that the

synthesis of silver nanoparticles using biological route or plant Extracts is beneficial against the pathological conditions. The "green "methods for the synthesis of silver nanoparticles have grown to be an area of attention as conventional chemical methods are expensive and have toxicity issues. Therefore there has been a search for low-cost, safe, economical, reliable, and "green" approach for the formation of stable metal nanoparticles with controlled size and shape. Therefore synthesized the silver nanoparticles of *S. cumini* methanol seed extract (ScSNPs) [6, 9]. Green synthesis of *S. cumini* silver nanoparticles is advantageous over the physical and chemical methods as it is ecofriendly and cost effective method due to avoidance of use of high temperature, pressure, energy and toxic chemicals [10, 14]. The bioreduction of Ag+ to Ag-NPs involves plant extracts such as *S. cumin* which are novel approach in *in vitro* cardiacmyocytes studies. Therefore, nanoparticles based the rapeutics may show a promising approach against diabetes induced complications. Here, we hypothesized that, silver nanoparticles containing *S. cumin* phyto nutrients may pass blood brain barrier and be less toxic to human cardiac cells (dose & time dependent manner). Despite of other diseases, the use of silver nanoparticles in the management of diabetic stress-induced cardiovascular diseases remains largely unexploited [9, 12]. These ScSNPs were characterized by UV-Vis spectrophotometer, X-ray diffract meter (XRD), scanning electron microscope (SEM), Zeta size, FTIR spectroscopy and their effect was observed on cardiac cell lines against glucose induced stress [11,14].

MATERIAL AND METHODS

Preparation of methanol seed extract of *Syzygium cumini*

10-15gm of leaves were weighed and sliced in to small pieces, and then 100-200ml of double distilled water was added and then boiled. After boiling the solution it is cooled. The extract was filtered with what man no.1 filter paper. The extract was stored at 4^{0c} for further usage. Required molar AgNO3 solution was prepared by accurate amount of silver nitrate was dissolved in required volume of water .generally for the preparation of silver nanoparticles we use 1mM silver nitrate solution. The solution was stored at dark color bottle for present to auto oxidation (0.0168g $AgNo_3$ /100ml D.W).

Green synthesis of silver nanoparticles

5 ml of methanol extract of *S. cumini* seeds was added to 95 ml of 0.1 M aqueous solution of silver nitrate in a flask, mixed gently and kept at room temperature for reduction into silver nanoparticles (AgNPs). After 48 hrs the solution turned from light to dark brown, indicating the formation of silver nanoparticles.

UV-Visible characterization

The synthesis of silver nanoparticles was characterized by UV-Visible spectra by using UV-Visible spectrophotometer (Shimadzu). Absorbance taken in UV and visible ranges provide the information regarding the plasmon resonance vibrations of silver ion in the extract. The silver nanoparticles were monitored at 400 to 450 nm in the UV-Visible spectrum.

SEM analysis

Scanning electron microscope (SEM) analysis elucidates the dimensions of the silver nanoparticles such as their surface, shape, and size. The extract solution containing silver nanoparticles was sonicated for 15 min at room temperature. The sample was diluted with double distilled water and a very small proportion was dropped on carbon coated copper grid, followed by drying for 5-10 min and the images were captured by SEM (Zeiss). The voltage, magnification and size were determined in images.

Determination of particle size and zeta potential analysis

The mean particle size (z-average) and zeta potential of ScSNPs were evaluated by Dynamic light scattering (DLS) using a zeta size analyzer (Nano ZS 90, Malvern Instruments Ltd., UK). The lyophilized dried powder was dissolved in water to obtain a proper scattering intensity.

X-Ray diffraction analysis (XRD)

XRD analysis determined the shape of silver nanoparticles; the powdered nanoparticles were coated on the amorphous silica substrate. The spectra were Recorded by using X-ray diffractometer with 40 kV and current of 30 mA with the radiation of Cu K (1.5418˚A) in a 2θ configuration. The crystallite size was Calculated from the width of the peaks, using the Scherrer formula as follows:

$$D = 0.94\lambda / \beta \cos \theta$$

Where D is the average crystallite domain size perpendicular to the reflecting planes, λ denotes X-ray wavelength (1.5418oA), β is the full width at half maximum (FWHM) and θ denotes diffraction angle.

Fourier transforms infrared spectroscopy (FTIR)

To identify the bio-molecules associated with the synthesis of nanoparticles by plant based methods, FTIR was performed by using FT-IR (Perkin Elmer Spectrum GX). The dried silver nanoparticles were measured at the wavelength range from 4000 to 400 cm-1.

In vitro antioxidant activities

DPPH assay

Equal volumes of extracts containing silver nanoparticles at various concentrations (0.2- 1 mg/ ml) were mixed with 0.135 mM DPPH prepared in methanol and Incubate in dark for 30 min [160]. The

absorbance was measured with UV –Vis spectrophotmeter at 517 nm against the control. The scavenging activity of extracts was calculated using the following equation:

$$\frac{OD_{Control} - OD_{sample}}{OD_{control}} * 100$$

Where OD control is the absorbance of DPPH + methanol; OD sample is the absorbance of DPPH radical + sample.

ABTS scavenging activity

For ABTS scavenging analysis, 7 mM ABTS solution and 2.4 mM potassium persulphate was mixed in equal proportion and incubated for 12-16 h at 25°C in the dark. Freshly prepared ABTS·+ solution (1 ml) was further added in the resulting mixture (161). Samples were mixed separately with the resulting mixture in 1:1 ratio After 10 min, the absorbance was measured at 734 nm. The quenching or inhibition capacity of the extracts for ABTS·+ and BHT was calculated by the equation as mentioned above.

Cellular uptake of silver nanoparticles

8x103 H9C2 cells were seeded on the coverslips and treated with 10 µg/ml concentration of silver nanoparticles, followed by incubation for 48 h. After fixing the cells with methanol, washing was done with 1X PBS. The film containing cover slip was allowed drying and the images were captured by SEM

MTT assay

Cell viability was measured by MTT, which was converted to purple formazan by the action of cellular enzymes present in the cytosol of living cells (205). For MTT Assay, 8x103 H9C2 cells were seeded in 96-well plates. After treatment with glucose and ScSNPs at different concentrations on cells, 10 µl MTT solution (5 mg/ml) was added and incubated at 25ºC for 3h. Formazan salt crystals were further dissolved in 100 µl dimethylsulfoxide (DMSO) and samples were analyzed at 570 nm. Cell viability is defined relative to untreated control cells as follows:

$$\frac{\text{Absorbance of treated sample - Absorbance of control}}{\text{Absorbance of control}} * 100$$

Morphological analysis by SEM

To observe the nanoparticles delivery in cell lines, H9C2 cells were treated in four experimental sets (i)Control H9C2 (Untreated) cells (ii)Cells induced with glucose(iii)Glucose induced cells treated with ScSNPs (iv)Cells treated with ScSNPs. The cells were visualized under SEM and ~ 50 times higher resolution images were captured.

Nuclear morphological analysis

DAPI staining

Cells of the above described experimental sets were fixed with methanol. DAPI (50ng/ml) dye was added in the cells and incubation was done for 15 min at 25°C. Cells were further observed under fluorescent microscope (Olympus Incorporation, Japan) using the DAPI filter at 40X magnification. The excitation and emission maxima for DAPI stain were found to be 435 and 495 nm respectively

PI Staining

Cells of the experimental sets were fixed with methanol and stained with PI (2.5ng/µl) solution for 15 min at 25°C in dark Cells were further observed under Fluorescent microscope using the TRITC filter and images were captured at 40X Magnification. The excitation/ emission maxima for PI stain was found to be 535/617 nm.

Lipid peroxidation assay

A modified thiobarbituric acid-reactive species (TBARS) assay (167) was performed with 100 µl cell suspension mixed with 10 µl acetic acid (pH adjusted to 3.5 with NaOH) and 150 µl of 0.8% (w/v) TBA in 1.1% sodium dodecyl sulphate and 0.5 µl.

20% TCA After cooling, 5.0 µl of butanol were added to each tube and centrifuged at 3000 rpm for 10 min. The absorbance of the organic upper layer was measured at 532nm by ELISA reader (Biorad). Inhibition of lipid peroxidation (%) by the sample was calculated.

Statistical Analysis

Statistical analysis was done by origin 8.5 software. A one-way ANOVA was used to evaluate the significance of the results obtained. All the results were significant at $P \leq 0.05$ level. Each experiment was conducted in triplicates.

RESULTS

As the *S. cumini* MSE was mixed with the silver nitrate solution, it was changed into dark brown color, which indicated the formation of silver nanoparticles (Figure-1). These nanoparticles were primarily subjected to UV-Vis spectroscopy and showed the peak of silver ion at 416 nm attributed to its surface plasmon resonance (Figure-2). Scanning electron microscopy revealed the size of silver nanoparticles, where averagely 40-100 nm sizes of nanoparticles were observed (Figure-3). Particle size distribution analysis also revealed the presence of around 40-100 nm of silver nanoparticles (Figure-4), however above 100 nm size of nanoparticles were also present in the powder, that may be due to the agglomeration of particles. After 6 months of duration,

the size and zeta potential was analyzed to know the stability of these *S. cumini* silver nanoparticles. The Z-average and zeta potential was found to be 43.02 nm and -19.6 mV respectively, which further confirms the stability of ScSNPs (Figure-5).

To further validate the synthesis of silver nanopartcles, XRD analysis was carried out which revealed the fundamental composition of nanoparticles as silver. The XRD pattern showed three diverse diffraction peaks at 38◦, 32◦ and 44◦ similar to diffraction from the 111, 101 and 200 planes of the cubic face centered silver and agrees with the literature (JCPDS no. 04-0783) (Figure-6). The average crystalline size was found to be ~ 45 nm as calculated by Sherrer equation.

The FTIR spectra in the region of 3000 to 450 cm revealed the presence of different functional groups. The 1700 cm-1 for C=O stretch, 1090 cm-1 for C-O stretch, 3737 and 3658 cm-1 contributes to hydrogen bonded O-H stretch (Figure-7). Peaks at the region of 3500-3100 cm-1, 2300-2200 cm-1 and 1610 cm-1 are disappeared in the spectra, indicates the absence of amines, nitriles and carbonyl groups respectively. Free radical (DPPH and ABTS•+) scavenging activities were estimated for ScSNPs and was compared with *S. cumini* MSE. Approximately 66% and 86% of inhibition Was observing by ScSNPs for DPPH and ABTS radicals respectively than that of *S.cumini* MSE and compared to standard gallic acid (GA) and butylated hydroxyl Toluene (BHT) (Figure-8). This indicated that silver nanoparticles have a potent antioxidant activity than that of *S. cumini* extract. An exact assessment of nanoparticles uptake is necessary for a better understanding of their action. Therefore, the uptake of silver nanoparticles was visualized by SEM analysis. Control cells treated with optimized dose of ScSNPs, after incubation of 48 hrs were visualized under scanning electron microscope. The nanoparticles in cardiac cells were observed at 3.07 times magnification, further 49.84 times and 51.95 times magnification showed a clear view of cells having nanoparticles of 44, 56 and 59 nm size (Figure-9).

The safe dose of *S. cumini* MSE silver nanoparticles was optimized by MTT assay and 20µg/ml dose was selected (Figure-10). Morphological analysis by electron Microscope revealed the increase in cell size after glucose administration, and the Treatment of stress cells with ScSNPs decrease the stress level by reducing the cell size upto control. Nuclear morphology was determined by DAPI and PI staining which showed the nuclear enlargement on glucose administration, and on combination with ScSNPs the morphology of nucleus remained intact.

The lipid peroxides formation was found to be increased up to two fold in glucose Stressed cells as compared to control cells; however on the treatment of ScSNPs and *S. cumini* separately in glucose stressed cells, the inhibition was reduced by 1.5 fold comparable to stressed cells.

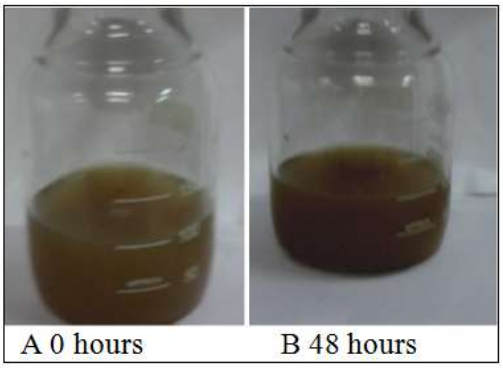

Fig-1: Colour change. (A) Mixture of *S. cumini* methanol extract + silver nitrate solution Yellowish colour (B) Change in colour as dark brown after 48 h of reaction indicating the formation of silver nanoparticles

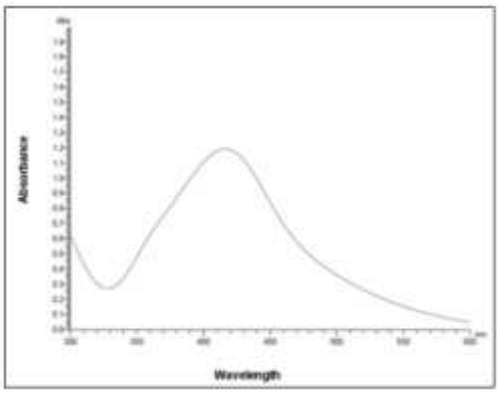

Fig-2: UV -Visible spectroscopy. The spectra denoting peak at 416 nm of silver nanoparticles of *S. cumini* MSE

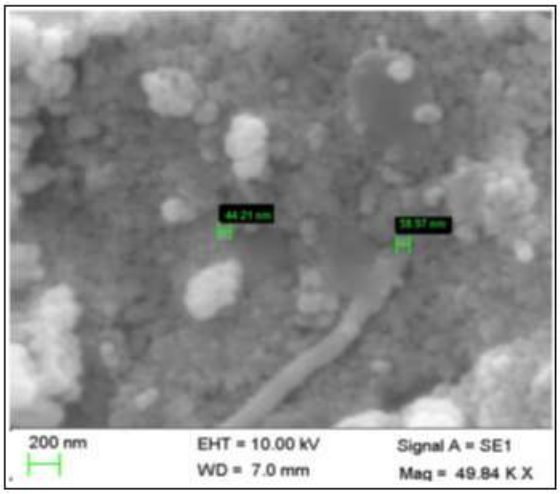

Fig-3: SEM Analysis. SEM analysis revealed the nanoparticles in a range of 40-100 nm. The silver nanoparticles containing extract was sonicated for 15 min at room temperature. A very small proportion was dropped on carbon coated copper grid, followed by drying for 5-10 min and the images were captured by SEM

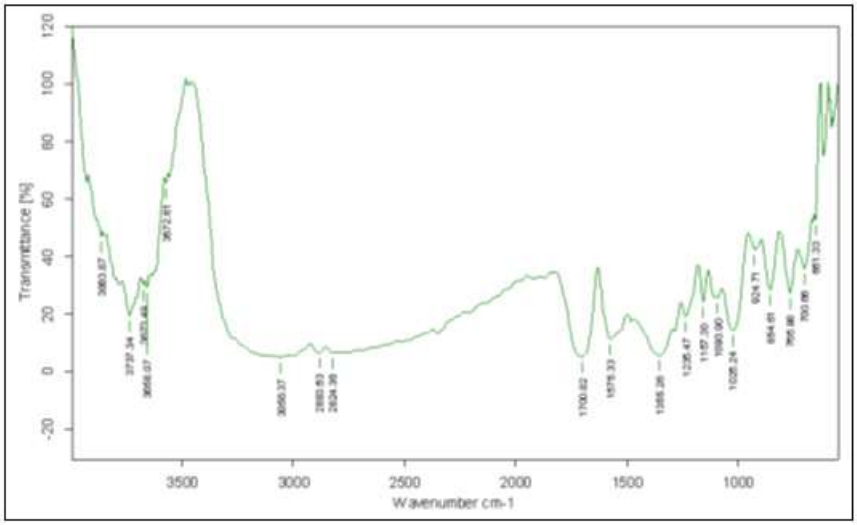

Fig-4: FTIR spectra of methanol extracted *S. cumini* silver nanoparticles. The FTIR spectra showed the absence of peaks at the region of 3500-3100 cm-1, 2300-2200 cm-1 and 1610 cm-1 in the spectra, indicates contribution of amines, nitriles and carbonyl groups respectively in silver nanoparticles formation

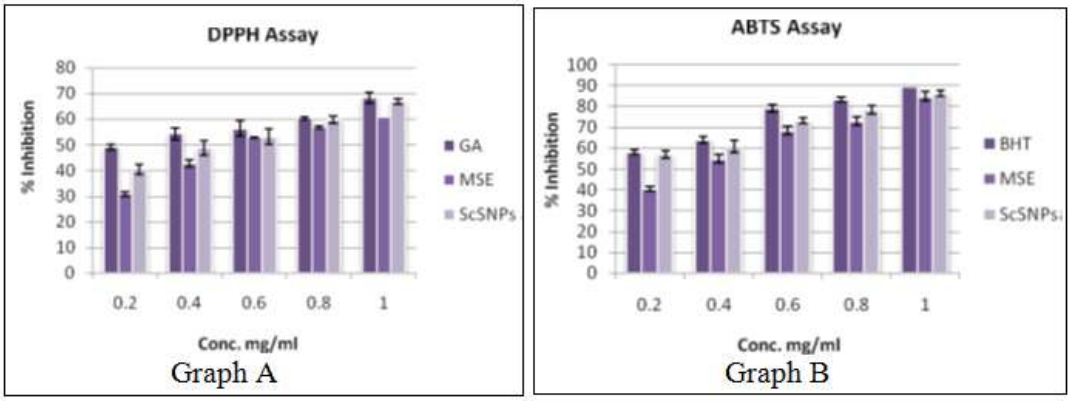

Fig-5: (A) DPPH Assay (B) ABTS assay. ScSNPs showed highest inhibition for DPPH and ABTS as compared to *S. cumini* MSE. MSE and ScSNPs showed the dose dependent inhibition for both of the radicals

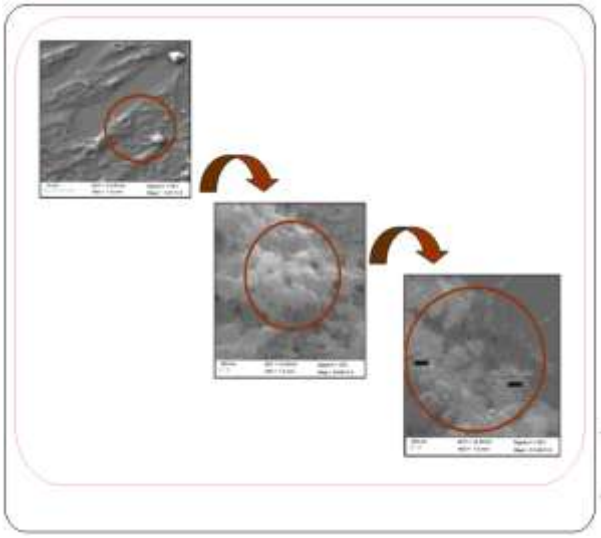

Fig-6: Uptake of ScSNPs in H9C2 cells. H9C2 cells were seeded on the cover slips and treated with 10 µg/ml concentration of silver nanoparticles, followed by incubation for 48 h. After fixing the cells with methanol, washing was done with 1X PBS. The images were captured by SEM

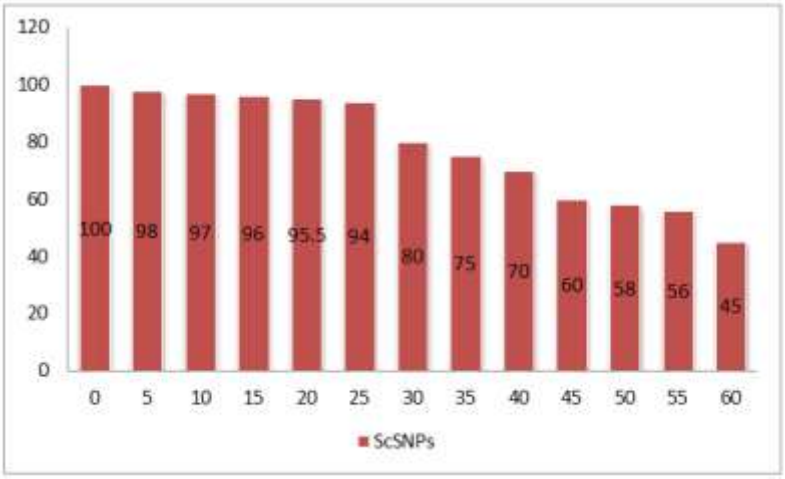

Fig-7: Dose optimization of ScSNPs was based on the production of formazan. Optimized dose was found to be 20 µg/ml for *S. cumini* silver nanoparticles

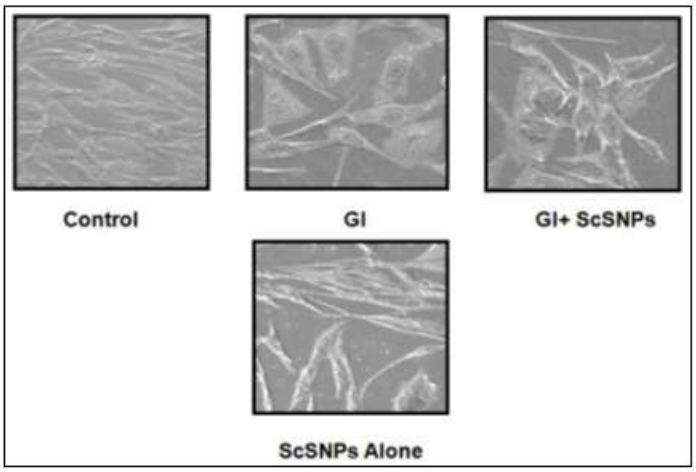

Fig-8: Morphological analysis of H9C2 cells on ScSNPs treatment by SEM analysis
Control (2) GI (3) GI+ ScSNPs (4) ScSNPs alone. Glucose induced cell showed the increase in cellsize whereas ScSNPs treatment reverses the cell size nearby control cells. ScSNPs alone treatment have shown no toxicity on cardiac cells

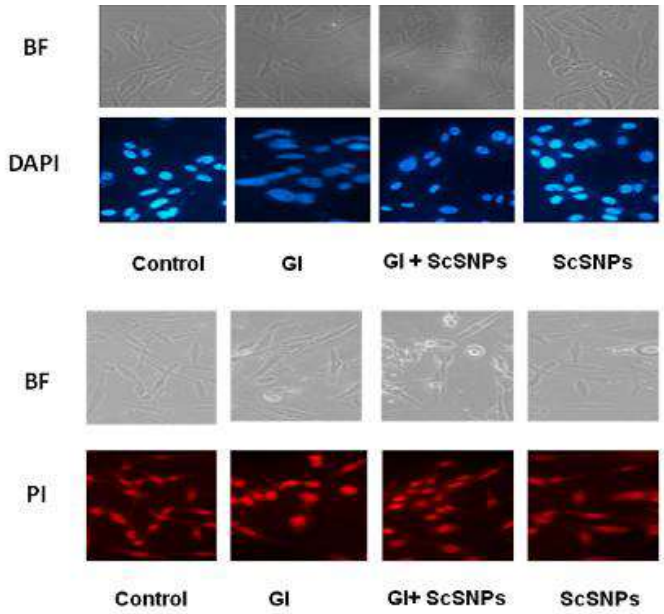

Fig-9: DAPI and PI staining in H9C2 cells. The increase in nuclear size was observed in Glucose induced cells however ScSNPs decrease the nuclear size upto control cells. Scale bar- 10 µM

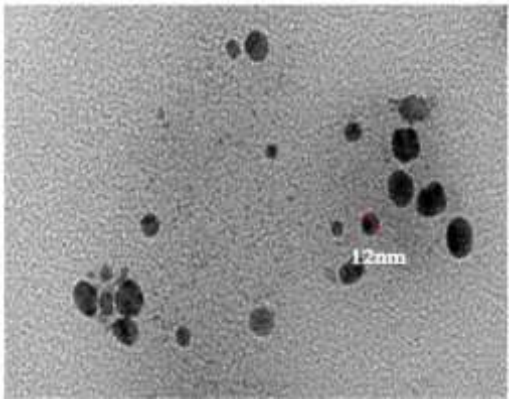

Fig-10: TEM analysis of s. cumini

DISCUSSION

The UV absorption spectra showed the peak at 416 nm of plasmon resonant silver nanoparticles. Plasmon resonance related with nanoparticle is dependent on the particle's size, shape, dispersity, material composition, surface area and local environment. The particle size distribution of the ScSNPs have shown the nanoparticles having 40 - 100 nm range, however greater than 100 nm size of Nanoparticles indicated their agglomeration, High resolution images of measured scattered electrons of sample for size distribution of nanoparticles. The synthesized ScSNPs were well distributed relating to intensity. Though it was not planned experimentally but we got a chance incidentally during a technological update to measure the size and zeta potential of our ScSNPs after six months of their preparation. To our surprise *S. cumini* synthesized silver nanoparticles were found to be stable even after 6 months. The particle size analysis and zeta potential Measurements showed 43.02 nm (84 % intensity) diameters with a zeta potential -21.8 mV, confirming that our ScSNPs were stable for long duration even at room Temperature. Therefore our study suggests that these nanoparicles are fairly stable at prolonged storage.

To determine the crystal structure and crystallite size, X-ray diffraction pattern gives a clear confirmation of silver nanoparticles, which are portrayed by the interplanar dspacing and the relative intensities (I/I0) of the intense peaks in sample. The fingerprinting region illustrates the relative intensity with respect to d-spacing values. For smaller nanoparticles (≤10-15 nm) the crystalline size closely Equivalent with respective particle size. However, for the larger nanoparticles the crystallite size was found to be less than the particle size (≥30 nm) due to multiple domain diffraction caused by crystal-twinning.

CONCLUSION

Our study showed the potential role of ScSNPs against glucose induced cardiac stress and need to be

explored further for mechanistic studies. The time dependent study should to be conducted in future to address the toxicity issues of nanoparticles *invitro* or *invivo*. Elucidation of mechanism behind phytosynthesis of precious metal nanoparticles is required in order to develop a coherent approach. In the current situation nanotechnology inspires the phytosynthetic path of nanoparticles synthesis, and will emerge as a safe and best alternative to conventional methods. Understanding the mechanism of silver nanoparticles functioning in depth is required along with the heightening and advancement of plant based synthesis of silver nanoparticles than that of conventional methods.

REFERENCE

1. Vidyasagar, G. M. (2014). Green synthesis, characterization and antimicrobial activity of Silver Nanoparticles by using Sterculia foetida L. young leaves aqueous extract.
2. Yang, X. (2016). *A study on antimicrobial effects of Nanosilver for drinking water disinfection*. Springer.
3. Awwad, A. M., & Salem, N. M. (2012). Green Synthesis of Silver Nanoparticles byMulberry LeavesExtract. *Nanoscience and Nanotechnology*, *2*(4), 125-128.
4. Banerjee, P., Satapathy, M., Mukhopahayay, A., & Das, P. (2014). Leaf extract mediated green synthesis of silver nanoparticles from widely available Indian plants: synthesis, characterization, antimicrobial property and toxicity analysis. *Bioresources and Bioprocessing*, *1*(1), 3.
5. Panigrahi, T. (2013). *Synthesis and characterization of silver nanoparticles using leaf extract of Azadirachta indica* (Doctoral dissertation).
6. Ali, Z. A., Yahya, R., Sekaran, S. D., & Puteh, R. (2016). Green synthesis of silver nanoparticles using apple extract and its antibacterial properties. *Advances in Materials Science and Engineering*, *2016*.
7. Kaviya, S., Santhanalakshmi, J., & Viswanathan, B. (2011). Green synthesis of silver nanoparticles using Polyalthia longifolia leaf extract along with D-sorbitol: study of antibacterial activity. *Journal of nanotechnology*, *2011*.
8. Seeram, H., Santhosh, K. J., Sravani, D. A., Ravi Kumar, G. A, Madhu, C. H. A., Susheela, B., Seeram, G. A., & Hariprasad. (2015). Green Synthesis, Characterization and Anti Microbial Activity of Silver Nano Particles. *International Journal of Engineering Research and Applications*, 5(10), 30-34.
9. Anandalakshmi, K., & Venugobal, J. (2017). Green Synthesis and Characterization of Silver Nanoparticles Using Vitex negundo (Karu Nochchi) Leaf Extract and its Antibacterial Activity. *Med. Chem.*, *7*, 218-225.
10. Ahmad, N., & Sharma, S. (2012). Green synthesis of silver nanoparticles using extracts of Ananas comosus. *Green and Sustainable Chemistry*, *2*(4), 141-147.
11. Anandalakshmi, K., Venugobal, J., & Ramasamy, V. (2016). Characterization of silver nanoparticles by green synthesis method using Pedalium murex leaf extract and their antibacterial activity. *Applied Nanoscience*, *6*(3), 399-408.
12. Geraldes, A. N., da Silva, A. A., Leal, J., Estrada-Villegas, G. M., Lincopan, N., Katti, K. V., & Lug&atildeo, A. B. (2016). Green nanotechnology from plant extracts: synthesis and characterization of gold nanoparticles. *Advances in Nanoparticles*, *5*(03), 176-185.
13. Kumar, R., Ghoshal, G., Jain, A., & Goyal, M. (2017). Rapid Green synthesis of silver nanoparticles (AgNPs) using (Prunus persica) plants extract: Exploring its antimicrobial and catalytic activities. *J Nanomed Nanotechnol*, *8*(452), 2.
14. Tran, Q. H., & Le, A. T. (2013). Silver nanoparticles: synthesis, properties, toxicology, applications and perspectives. *Advances in Natural Sciences: Nanoscience and Nanotechnology*, *4*(3), 033001.
15. Kim, S. H., Lee, H. S., Ryu, D. S., Choi, S. J., & Lee, D. S. (2011). Antibacterial activity of silver-nanoparticles against Staphylococcus aureus and Escherichia coli. *Korean J. Microbiol. Biotechnol*, *39*(1), 77-85.
16. Ghotekar, S. K., Pande, S. N., Pansambal, S. S., Sanap, D. S., Mahale, K. M., & Sonawane, B. (2015). Biosynthesis of silver nanoparticles using unripe fruit extract of Annona reticulata L. and its characterization. *World J. Pharm. and Pharm. Sci*, *4*(11), 1304-1312.
17. Diptendu, S., & Goutam, P. (2017). Green Synthesis of Silver Nanoparticles Using Mentha Asiatica (Mint) Extract and Evaluation Of Their Antimicrobial Potential. *International Journal of Current Research in Biosciences and Plant Biology*, 4.
18. Baishya, D., Sharma, N., & Bora, R. (2012). Green synthesis of silver nanoparticle using Bryophyllum pinnatum (Lam.) and monitoring their antibacterial activities. *Archives of Applied Science Research*, *4*(5), 2098-2104.